ADVANCED MATERIALS

rameter variation, i.e., different metals, well-defined initial concentration of carbon and metal, etc. Therefore, it may be a useful instrument for clarifying growth mechanisms of carbon nanotubes and graphite-encapsulated nanoparticles.[27]

If the yield of tubes can be increased and their structure can be tailored by parameter variations, nanotube production might become cheaper and products from nanotubes might come within closer range.

Received: July 1, 1998
Final version: September 7, 1998

[1] S. Iijima, *Nature* **1991**, *354*, 56.
[2] C. H. Klang, M. S. de Vries, G. Gorman, R. Savoy, J. Vazquez, R. Beyers, *Nature* **1993**, *363*, 605.
[3] T. W. Ebbesen, *Carbon Nanotubes*, CRC, Boca Raton, FL **1997**.
[4] M. S. Dresselhaus, G. Dresselhaus, P. C. Eklund, *Science of Fullerenes and Carbon Nanotubes*, Academic Press, San Diego, CA **1996**, Ch. 19.
[5] E. W. Wong, P. E. Sheehan, C. M. Lieber, *Science* **1997**, *277*, 1971.
[6] S. J. Tans, A. R. M. Verscheuren, C. Dekker, *Nature* **1998**, *393*, 49.
[7] T. W. Ebbesen, P. M. Ajayan, *Nature* **1992**, *358*, 220.
[8] L. A. Chernozatonskii, Z. Ja. Kosakovskaja, E. A. Fedorov, V. I. Panov, *Phys. Lett. A* **1995**, *197*, 40.
[9] M. Ge, K. Sattler, *Science* **1993**, *260*, 515.
[10] M. Endo, K. Takeuchi, S. Igarashi, K. Kobori, M. Shiraishi, H. W. Kroto, *J. Phys. Chem. Solids* **1993**, *54*, 1841.
[11] N. Hatta, K. Murata, *Chem. Phys. Lett.* **1994**, *217*, 398.
[12] M. Terrones, N. Grobert, J. Olivares, J. P. Zhang, H. Terrones, K. Kordatos, W. K. Hsu, J. P. Hare, P. D. Townsend, K. Prassides, A. K. Cheetham, H. W. Kroto, D. R. M. Walton, *Nature* **1997**, *388*, 52.
[13] S. Iijima, T. Ichihashi. *Nature* **1993**, *363*, 603.
[14] C. Journet, W. K. Maser, P. Bernier, A. Loiseau, M. Lamy de la Chapelle, S. Lefrant, P. Deniard, R. Lee, J. E. Fischer, *Nature* **1997**, *388*, 756.
[15] W. K. Hsu, J. P. Hare, M. Terrones, H. W. Kroto, D. R. M. Walton, P. J. F. Harris, *Nature* **1995**, *377*, 687
[16] P. M. Ajayan, T. W. Ebbesen, *Rep. Prog. Phys.* **1997**, *60*, 1025.
[17] A. I. Liumkin, E. A. Petrov, A. P. Erskov, *Sov. Phys.-Dokl.* **1988**, *302*, 611.
[18] V. L. Kuznetsov, A. L. Chuvilin, E. M. Moroz, V. L. Kalomiichuh, Sh. K. Shaikhutinov, Yu. V. Butenko, I. Yu. Mulkov, *Carbon* **1994**, *32*, 873.
[19] S. Eidelmann, A. Altshuler, *Nanostruct. Mater.* **1993**, *3*, 31.
[20] R. Boese, A. J. Matzger, K. P. C. Vollhardt, *J. Am. Chem. Soc.* **1997**, *119*, 2052.
[21] A. C. Frank, F. Stowasser, H. Sussek, H. Pritzkow, C. R. Miskys, O. Ambacher, M. Giersig, R. A. Fischer, *J. Am. Chem. Soc.* **1998**, *120*, 3512.
[22] E. Ott, E. Ohse, *Chem. Ber.* **1921**, *54*, 179.
[23] J. Kähler, E. Meyer, *Explosivstoffe*, 8th ed., VCH, Weinheim **1995**.
[24] X. X. Zhou, Y. Z. Yu, *Kogyo Kayaku* **1991**, *52*, 251.
[25] C. Guerret-Piecourt, Y. L. Bouar, A. Loiseau, H. Pascard. *Nature* **1994**, *372*, 761.
[26] Ref. [3], page 267.
[27] B. R. Elliott, J. J. Horst, V. P. David, M. H. Teng, J. H. Hwang, *J. Mater. Res.* **1997**, *12*, 3328.

Elastic Modulus of Ordered and Disordered Multiwalled Carbon Nanotubes**

By *Jean-Paul Salvetat*,* *Andrzej J. Kulik*, *Jean-Marc Bonard*, *G. Andrew D. Briggs*, *Thomas Stöckli*, *Karine Méténier*, *Sylvie Bonnamy*, *François Béguin*, *Nancy A. Burnham*, and *László Forró*

Carbon nanotubes[1] are predicted to have not only fascinating electrical but also remarkable mechanical properties. Experimental evidence confirms that they can be stiff elastic rods of very low density,[2–4] which show unique mechanical properties and so are ideal candidates for high performance composites. Multiwall nanotubes (MWNTs) are usually produced by the arc-discharge method, providing nearly perfect structures consisting of nested graphene cylinders.[5] Point defects may be present on the graphitic planes, but they should be removed to a great extent by high-temperature annealing. Another way of producing MWNTs is by thermal decomposition of hydrocarbons in the presence of catalysts.[6] The advantage of this catalytic process is that it can yield an almost continuous production of long nanofibers. However, catalytic reactions may produce only partially ordered nanotubes containing structural defects, which are expected to lower their mechanical properties. We report here on elastic measurements on as-grown and annealed arc-discharge nanotubes (the latter having a lower point defect density than the former), and on disordered catalytic nanotubes. We found that although the elastic properties of the nanotubes are scarcely affected by the presence of point defects, extended stacking defects and disorder can reduce the elastic modulus by orders of magnitude.

The arc-discharge carbon nanotubes were produced in a carbon arc apparatus using the method described by Ebbesen and Ajayan.[5] They consist of nested graphitic cylinders that are perfectly aligned with the tube axis, as can be seen in the transmission electron microscopy (TEM) image of Figure 1a. The nanotubes were obtained from the raw soot after separation from nanoparticles and larger graphitic objects by means of a soft purification method that yields nearly pure nanotube samples without any damage to the

[*] Dr. J.-P. Salvetat, Dr. A. J. Kulik, Dr. J.-M. Bonard, Dr. T. Stöckli, Dr. N. A. Burnham, Dr. L. Forró
Département de Physique, Ecole Polytechnique Fédérale de Lausanne
CH-1015 Lausanne (Switzerland)
Prof. G. A. D. Briggs
Department of Materials, Oxford University
Parks Road, Oxford OX1 3PH (UK)
Dr. K. Méténier, Dr. S. Bonnamy, Prof. F. Béguin
CNRS/CRMD
F-45071 Orléans Cedex 2 (France)

[**] We thank G. Beney (EPFL) for polishing the filters, as well as the CIME-EPFL for access to the electron microscopes. This work was supported by the Swiss NSF.

  0935-9648/99/0201-0161 $ 17.50+.50/0

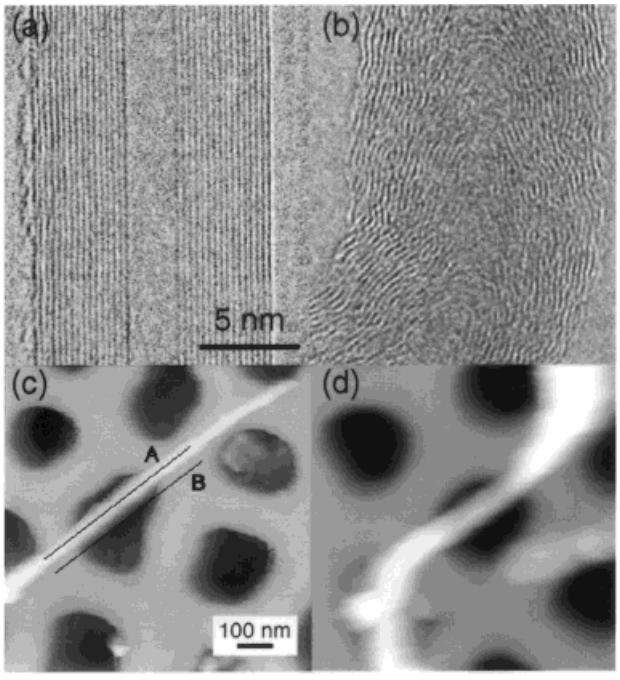

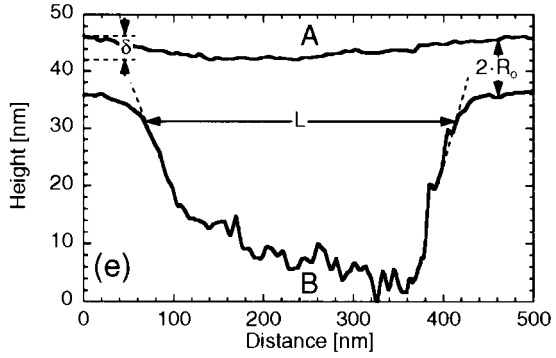

Fig. 1. a,b) TEM images of typical nanotubes. c,d) AFM images of nanotubes adhered on the polished ultrafiltration alumina membrane with a portion bridging a pore of the membrane. a,c) For an arc-discharge MWNT; b,d) for a catalytic MWNT. e) Cross-sectional profiles of the nanotube (A) and corresponding pore (B) depicted in (c).

graphitic walls.[7] Furthermore, since point defects are believed to be present in as-grown MWNTs,[8] arc-grown tubes were also studied after high temperature annealing at 2500 °C to investigate the influence of the reduced point defect density on the elastic modulus.

The disordered nanotubes were produced by catalytic decomposition of acetylene on reduced cobalt oxide that was deposited on a silica substrate.[9] The nanotube powder was collected after dissolution of the silica substrate in HF and the catalyst in HNO. In this case, the nanotubes show a high density of structural defects.[10] As displayed in the TEM image of Figure 1b, the planes are typically tilted with an angle about 30° with respect to the tube axis, forming a piled-up 'coffee-cup' structure. For both types of tubes, the purified nanotube powder was dispersed in chloroform by mild sonication.

One method for measuring the elastic modulus of a material is to fabricate a beam that is subsequently clamped at each end (or, alternatively, left simply supported) and to measure its vertical deflection versus the force applied at a point midway along its length.[11] The atomic force microscope (AFM) naturally suggests itself as a means to study the mechanical properties of nanotubes, since it allows one to measure the deflection of a sample as a function of the applied force when used in the contact mode. However, there remains the problem of configuring a nanotube suspended over an empty space. Our solution is to deposit a droplet of the nanotube suspension on a well-polished alumina ultrafiltration membrane (Whatman Anodisc, with 200 nm pores). On such a substrate, nanotubes occasionally lie over the pores, either with most of the tube in contact with the membrane surface as in the AFM images of Figures 1c and 1d, or with the tube suspended over a succession of pores. The attractive interaction between the nanotubes and the membrane acts to clamp the tubes to the substrate. Hence, we selected tubes with long lengths in contact with the membrane and assumed that they were rigidly clamped. This assumption will be discussed in detail later on.

We used an AFM (M5 Park Scientific Instruments in contact mode) operating in air and equipped with closed loop feedback for accurate scanner positioning. For the AFM tip we tried both Si_3N_4 and Si cantilevers with different force constants (between 0.05 and 0.26 N/m). Once a suspended nanotube had been located with the AFM we determined its diameter, suspended length, and deflection midway along the suspended length from data like those of Figure 1e, which show cross-sectional profiles of the nanotube (profile A) and corresponding pore (profile B) depicted in Figure 1c. The apparent tube width is a combination of the tube diameter and the tip radius and hence gives only a poor estimate of the actual tube diameter. Alternatively, the height remains a reliable measure of the tube diameter as long as its radial deformation by adhesive forces and/or applied load are negligible, which should be the case for a MWNT[12] as discussed below. As for the suspended length, it is apparent in profile B of Figure 1e that the edges of the pores are slightly rounded. The suspended length is taken here as the distance between the beginning of the shoulders as denoted by L in Figure 1e, and represents thus a lower limit of this parameter.

A typical deflection (δ) versus applied force (F) measurement is shown in Figure 2. The reversibility of the tube deflection and the linearity of the δ–F curve show that the nanotube response is linear and elastic for this range of forces.

The deflection δ of an isotropic beam as a function of the applied load is known from small deformation theory to be given by Equation 1, where F is the applied force, L is the suspended length, E is the elastic modulus, I is the second moment of area of the beam (usually called moment of inertia), and $\alpha = 192$ for a clamped beam and 48 for a simply

0935-9648/99/0201-0162 $ 17.50+.50/0

ADVANCED MATERIALS

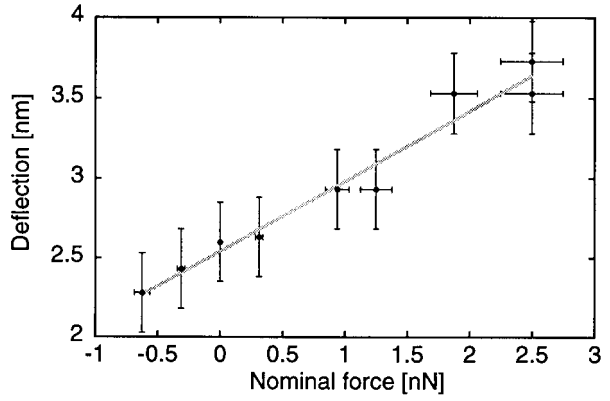

Fig. 2. Deflection δ versus applied force F for an arc-discharge MWNT (No. 2, see Table 1). The suspended length was $L = 350^{+40}_{-4}$ nm, and the diameter of the tube was 10±0.5 nm. For the range of forces applied, the response of the nanotube was linear and elastic, i.e., reversible. The solid line is a linear regression fit of the experimental data, with a slope inversely proportional to the elastic modulus. Note that it does not pass through the origin of the graph. The rounded surface between the pores induces a deflection of the tubes even without any applied force, and the absolute value of the force is not the nominal force applied by the tip due to attractive forces between tip and sample.

supported beam.[11] For a hollow cylinder, $I = \pi(R_o^4 - R_i^4)/4$, R_o and R_i being respectively the outer and inner radii.

$$\delta = FL^3/(\alpha EI) \quad (1)$$

Because the absolute values of force and deflection are not known, we measured the change in deflection as a function of the change in load. Using Equation 1, the slope of the curve (typically 0.5 m/N) directly gives the elastic modulus of the MWNT once L and R_o are known.

As displayed in Table 1, we determined the elastic modulus for eleven individual arc-grown carbon nanotubes (as-grown and annealed). We found no significant correlation between E and the diameter of the tube. Furthermore, there is no apparent difference between annealed and unannealed nanotubes. This suggests that point defects, if present at all, do not alter the mechanical properties of MWNTs. The average value of the elastic modulus for the arc-discharge MWNT is 810^{+410}_{-160} GPa. This is in strong contrast with the values measured for five catalytic nanotubes: the elastic modulus ranges from 10 to 50 GPa. The disorder present in catalytic nanotubes thus influences considerably the elastic properties.

The error we quote in the results is the probable error, and is largely due to the strong dependence of δ on the radius and suspended length of the nanotubes as measured with the AFM. The error in the diameter is typically ±0.5 nm, i.e., ±5 %. It amounts to $^{+10}_{-1}$ % for the suspended length, since we extract the lower limit for this parameter from our AFM profiles, as discussed above. A further source of error arises from the uncertainty in the inner diameter of the tube, which cannot be measured by AFM. An extensive TEM study by Bacsa et al. on arc-grown

Table 1. Outer radius R_o, suspended length L, and elastic modulus E for the multiwall nanotubes studied in this work. Nanotubes 1–5 and 6–11 are as-grown and annealed arc-discharge MWNTs, respectively. Nanotubes 12–16 are catalytic MWNTs. All tubes but No. 11 behaved as clamped beams, i.e., the tube length in contact with the substrate was at least 200 nm. Nanotube 11, with only 20 nm of its length in contact on both sides of the pores, was taken to be simply supported.

Nanotube No.	R_o [nm] ±5 %	L [nm] +10 %, –1 %	E [GPa] +50 %, –20 %
1	4.8	280	860
2	5.0	350	1100
3	5.5	250	760
4	6.0	280	670
5	6.5	240	980
Average, as-grown MWNTs	–	–	870
6	5.0	310	830
7	6.0	300	830
8	7.0	420	720
9	7.5	400	810
10	8.0	390	600
11	10.0	360	740
Average, annealed MWNTs	–	–	755
Average, arc-discharge MWNTs	–	–	810
12	15.0	240	17
13	14.0	260	22
14	16.0	240	35
15	13.0	210	50
16	13.0	280	12
Average, catalytic MWNTs	–	–	27

MWNTs[13] demonstrated that it can vary from 1 to 6 nm for a tube of 10 nm outer diameter, with the most probable value being ~2 nm. We chose to assume $R_i = 1$ nm, with the consequence that we calculate the minimum value for E. If in fact the inner diameter were 6 nm, the resulting error would be +13 %, less than our probable error of +50 %. In the case of the disordered nanotubes, the error is larger since the diameter is not constant along the suspended portion. We applied the clamped beam formula for a mean value of the diameter, and it is possible that the calculated modulus is underestimated, since the stress induced by the applied load is not homogeneously distributed. However, we selected suspended portions that appeared as uniform as possible by AFM to minimize this source of error.

MWNTs are expected to be anisotropic in their elastic properties. For ordered arc-grown tubes, the radial elastic constant c_{11} was calculated to be about one-third of the axial elastic constant c_{33}.[14] Our values could therefore be influenced by compression along the axis of the tip and radial compression of the nanotube directly beneath the tip in addition to the flexion of the entire beam. An estimate for the compliance of the tip–tube contact is $(6F\tilde{R}E^{*2})^{-1/3}$, where F is the load, $\tilde{R}$ is the local radius of curvature and

  0935-9648/99/0201-0163 $ 17.50+.50/0

E^* is the reduced elastic modulus of the tip and sample.[15] Taking these quantities to be 5 nN, 10 nm, and 200 GPa, respectively, the compliance is 4.4×10^{-3} m/N, two orders of magnitude less than the slope in Figure 2. Thus the local tip/tube compression should not affect our results. This can be verified experimentally by checking that the tube height and width measured on the substrate do not vary when the applied force is increased. We were especially careful with catalytic nanotubes, for which the elastic constant should be much lower.

In checking further the validity of our method, we must emphasize that the most tenuous assumption concerns the hypothesis of the clamped beam. The question is whether the adhesion forces are strong enough to prevent nanotubes from lifting off the substrate. The first qualitative argument is that due to large lateral forces exerted by the cantilever, the nanotubes would be dragged away by the tip in the absence of strong adhesion. We found that we could reproducibly image the tubes in contact mode. For the most rigid cantilever, images of the suspended portion of the tubes obtained with left-to-right scans differed markedly from the complementary right-to-left scan images, while no significant differences were detected on the parts lying on the substrate. A lateral bending of the suspended parts of the nanotubes was therefore observed for lateral forces that we estimate to a few hundred nanonewtons, i.e., an order of magnitude higher than the normal forces applied by the tip. Another argument in favor of the clamped beam assumption is given by the interesting case of nanotube No. 11 (see Table 1). It was suspended over a line of three pores with only 20 nm of its length touching each rim of the central pore (not shown here). For the section of the tube that bridged the middle hole, we applied the formula for the simply supported beam with $\alpha = 48$ in Equation 1. Had we used $\alpha = 192$ (i.e., clamped beam), the resulting value for E would have fallen well below the other ten, for which at least 200 nm of the tube length was in contact with the membrane.

The average elastic modulus measured on ordered arc-grown MWNTs is consistent with the in-plane elastic constant of graphite, $c_{11} = 1.06$ TPa,[16] and with simulations using the force-constant model.[14] Our results are furthermore compatible with the values obtained in previous studies (0.4–3.7 TPa[2] and 1.26±0.59 TPa[3]). The insignificant effect of the annealing at 2500 °C on the elastic properties was also expected for it is known from studies of neutron irradiation effects that c_{11} is not affected by a low concentration of vacancies and interstitials.[17] Our results confirm that the elastic modulus cannot be much higher for arc-grown MWNTs than that expected from macroscopic graphite since the curvature of the graphitic planes is not high enough to induce stiffening if their diameters exceed 2 nm.[14,18]

In contrast, the elastic behavior of disordered nanotubes may involve shear deformation, which is sensitive to defects and dislocations.[16] For a perfect graphite crystal, the shear modulus c_{44} equals 4.5 GPa as measured from thermal properties but it can be as low as 0.18 GPa for pyrolytic graphite due to glissile basal plane dislocations.[19] As a rough approximation, we will consider a catalytic nanotube as a graphite cylinder where the graphitic planes show an angle ϕ with respect to the tube axis. The variation of the elastic modulus with ϕ in a single graphite crystal is given by Equation 2, where S_{ij} are the elastic compliances of bulk graphite and $\gamma = \sin(\phi)$.[16]

$$1/E = S_{11}(1-\gamma^2)^2 + S_{33}\gamma^4 + (2S_{13} + S_{44})\gamma^2(1-\gamma^2) \quad (2)$$

Owing to the strong anisotropy of graphite, and especially to the low value of c_{44} as compared to the other elastic constants, Equation 2 can be simplified to $1/E \approx S_{44}\gamma 2(1-\gamma^2)$ when ϕ is less than 45°. (Note that $S_{44} = 1/c_{44}$.) When $\phi = 10°$, E is about $34c_{44}$ (≈150 GPa), whereas it drops to $5c_{44}$ (≈20 GPa) when $\phi = 30°$. Very high modulus fibers are achieved only when extended stacks of graphitic planes are well aligned in the fiber axis direction, which is the case here for arc-grown nanotubes. The decrease of the modulus for catalytic nanotubes seems therefore to be mainly due to the misalignment of the graphitic planes with the tube axis and the large dispersion in the measured modulus reflects the large sensitivity of E to the structural order.

Larger fibers grown by similar catalytic chemical vapor deposition (CCVD) methods usually show higher moduli. We suspect that this arises from the structural morphology of the fibers, i.e., from the high degree of preferential orientation of the graphitic planes parallel to the fiber axis.[20] Moreover, from the experimental values of E (between 10 and 50 GPa), we can deduce from the above considerations that the shear modulus cannot be much lower than 1 GPa for the catalytic tubes. This value is higher than in pyrolitic graphites.[19] We speculate that in our case, glissile dislocations are pinned by defects and/or shear deformation is blocked by disorder in graphitic plane stacking. Note that annealing of catalytic disordered tubes at 2500 °C yields well-ordered MWNTs with a structure similar to those obtained by arc-discharge. Measurements performed on such samples revealed a strong increase in the elastic modulus of at least one order of magnitude. Unfortunately, the deflections were too small to be measured with the present method because of the large tube diameter.[21]

In conclusion, we have used a miniaturized beam configuration to establish directly a minimum value of the elastic modulus for carbon nanotubes. E ranged between 10 and 50 GPa for disordered catalytic nanotubes, which is consistent with the elastic anisotropy of bulk graphite and with the structural disorder of these tubes. Catalytic nanotubes are more suited for large scale applications, but our results show that special care is needed to produce highly ordered nanotubes, because structural defects may considerably reduce their mechanical properties. For the structurally ordered nanotubes, the average modulus was 810^{+410}_{-160} GPa. Our AFM measurements thus confirm that arc-grown

  0935-9648/99/0201-0164 $ 17.50+.50/0

ADVANCED MATERIALS

nanotubes are the ultimate high modulus fibers predicted by theory.

Received: June 19, 1998
Final version: September 10, 1998

[1] S. Iijima, *Nature* **1991**, *354*, 56.
[2] M. M. J. Treacy, T. W. Ebbesen, J. M. Gibson, *Nature* **1996**, *381*, 678.
[3] E. W. Wong, P. E. Sheehan, C. M. Lieber, *Science* **1997**, *277*, 1971.
[4] M. R. Falvo, G. J. Clary, R. M. Taylor, II, V. Chi, F. P. Brooks, Jr, S. Washburn, R. Superfine, *Nature* **1997**, *389*, 582.
[5] T. W. Ebbesen, P. M. Ajayan, *Nature* **1992**, *358*, 220.
[6] M. José-Yacamán, M. Miki-Yoshida, L. Rendón, J. G. Santiesteban, *Appl. Phys. Lett.* **1993**, *62*, 657.
[7] J.-M. Bonard, T. Stora, J.-P. Salvetat, T. Stöckli, F. Maier, C. Duschl, W. A. de Heer, L. Forró, A. Châtelain, *Adv. Mater.* **1997**, *9*, 827.
[8] M. Kosaka, *Chem. Phys. Lett.* **1995**, *233*, 47.
[9] A. Hamwi, H. Alvergnat, S. Bonnamy, F. Béguin, *Carbon* **1997**, *35*, 723.
[10] It is worth noting that nanotubes with partly graphitized structure can be produced by catalytic reactions using slightly different growth conditions.
[11] J. M. Gere, S. P. Timoshenko, in *Mechanics of Materials*, PWS-KENT Publishing, Boston, MA **1990**.
[12] R. S. Ruoff, J. Tersoff, D. C. Lorents, S. Subramoney, B. Chan, *Nature* **1996**, *364*, 514.
[13] W. S. Bacsa, R. LaDuca, J. Hoerter, F. Chibante, S. Subramoney, J. G. Lavin, K. Parvin, R. S. Ruoff, in *Fullerenes*, Vol. 3 (Eds: K. M. Kadish, R. S. Ruoff), Electrochemical Society, Pennington, NJ **1996**.
[14] J. P. Lu, *Phys. Rev. Lett.* **1997**, *79*, 1297.
[15] J. B. Pethica, W. C. Oliver, *Phys. Scr.* **1987**, *19*, 61.
[16] B. T. Kelly, *Physics of Graphite*, Applied Science, London **1981**.
[17] E. J. Seldin, C. W. Nezbeda, *J. Appl. Phys.* **1970**, *41*, 3389.
[18] C. F. Cornwell, L. T. Wille, *Solid State Commun.* **1997**, *101*, 555.
[19] O. L. Blakslee, D. G. Proctor, E. J. Seldin, G. B. Spence, T. Weng, *J. Appl. Phys.* **1970**, *41*, 3373.
[20] M. S. Dresselhaus, G. Dresselhaus, K. Sugihara, I. L. Spain, H. A. Goldberg, *Graphite Fibers and Filaments*, Springer, Berlin **1988**.
[21] The catalytic tubes have a diameter about twice as large as the arc-produced tubes (see Table 1). The resulting deflections are then ~16 times smaller under the same conditions.

Synthesis of Photonic Crystals for Optical Wavelengths from Semiconductor Quantum Dots**

By *Yurii A. Vlasov*, *Nan Yao*, and *David J. Norris**

Even with modern nanolithography, fabrication of nanometer-scale materials that are patterned and highly ordered in three dimensions remains a challenge.[1–3] While lithographic methods are now capable of nanometer-scale resolution, they define features at an interface and are difficult to extend to three dimensions. To address this problem, self-organization has been explored as an alternative route to complex materials.[4] For example, porous solids have recently been prepared by infiltrating material into self-organized templates and then removing the template.[5–11] This technique has led to ceramic[5–10] and carbon[11] structures with highly ordered macropores (pores larger than 50 nm). Such solids have important implications as photonic crystals—artificial crystals where the size of the unit cell is comparable to the wavelength of the photon. Many novel properties have been predicted for photonic crystals, including the ability to control the flow of light.[12] However, since the latest self-organization methods[5–11] generate ceramic or carbon materials, the resulting macroporous solids cannot exploit the optical properties of conventional semiconductors (high refractive index, efficient luminescence, gain, and optical nonlinearities) on which many applications of photonic crystals rely. Although attempts have been made to fill self-organized templates with semiconductors such as CdS and InP,[13–16] the filling of the template was incomplete and macroporous semiconductor solids could not be obtained. A new method for producing semiconductor photonic crystals is required.

In this communication we show how to use self-organization to synthesize ordered, macroporous, semiconductor solids. We induce nanometer-scale semiconductor particles, or nanocrystals,[17–19] to self-assemble inside a self-organized silica template. Subsequently, the template is removed and a three-dimensionally patterned material consisting solely of densely packed nanocrystals is obtained. The resulting photonic crystal can utilize the properties of individual nanocrystals as well as their collective interactions.[20–22] Furthermore, the nanocrystals can be sintered to form a macroporous bulk semiconductor that has promise as a photonic bandgap material for optical wavelengths. Although we demonstrate only semiconductor structures, our method represents a general and inexpensive route to three-dimensionally patterned solids.

Our approach combines colloidal chemistry with two steps of hierarchical self-assembly. Colloidal silica particles are first used to construct a self-organized silica template. This template then serves as a three-dimensional scaffolding for the self-assembly of colloidal nanocrystals. After the template is filled with nanocrystals, the silica is removed by selective etching to yield a three-dimensionally patterned, porous solid. Since the template is removed at room temperature, we avoid shrinkage and distortion of the pores. Therefore, the exact three-dimensional structure of the template is imprinted in the final material.

While this procedure can utilize the large variety of materials that can now be prepared as nanocrystals, here we produce such solids using semiconductor nanocrystals (or quantum dots). The resulting material is particularly interesting as a photonic crystal since we control several important parameters that determine its final behavior. First, we control the individual nanocrystals. Due to their size, quantum dots exhibit optical and electronic properties dramatically different from both molecules and macroscopic sol-

[*] Dr. D. J. Norris, Dr. Yu. A. Vlasov
NEC Research Institute
4 Independence Way, Princeton, NJ 08540 (USA)
Dr. N. Yao
Princeton Materials Institute, Princeton University
70 Prospect Avenue, Princeton, NJ 08540 (USA)

[**] We thank E. Dujardin, T. Ebbesen, A. Krishnan, H. Stone, and M. Treacy for helpful discussions and assistance.

  0935-9648/99/0201-0165 $ 17.50+.50/0